COBEM 2021 26th International Congress of Mechanical Engineering
November 22-26, 2021, Virtual Congress, Brazil
ABCM Associação Brasileira de Engenharia e Ciências Mecânicas

COB-2021-0224
NUMERICAL MODELING OF FLUIDS MIXTURE FLOW IN HIGH VELOCITIES WITH PHASE CHANGE

Breno de Almeida Avancini
Bruno Souza Carmo
Department of Mechanical Engineering, Escola Politécnica, University of Sao Paulo.
Av. Prof. Mello Moraes, 2231 - Butantã, São Paulo - SP, Brazil 05508-030
breno.avancini@usp.br

Abstract. *The oil and gas industry raises the demand for new gas separation technologies due to the exploration of the pre-salt reservoirs where the natural gas have a high concentration of carbon dioxide. The sugar and ethanol industry also contributes to this demand with the increase of the production of biogas from vinasse, which also has a high CO_2 content. For this reason, we investigate the feasibility of using supersonic gas separators to remove part of the carbon dioxide content from raw natural gas and biogas. In that context, we have developed a model of the fluid flow behaviour in a nozzle which allows the verification of the supersonic nozzle separator performance in the component separation of fuel gases that contain high amounts of carbon dioxide and methane. The proposed model assumes inviscid one-dimensional compressible flow of a gas mixture with homogeneous nucleation and growth of CO_2 droplets. We implemented a partial differential equation solver of the set of equations that model the flow based on the AUSM scheme. We predicted the thermodynamic and physical properties of the fluids using expressions that consider non-ideal fluid behaviour and non-equilibrium states, such as metastability, and are readily available in computational libraries. First, validations of the numeric model were carried out, through the comparison of simulation results with experimental data of supersonic wet steam flows found in the literature. Next, we have produced a numerical model of the flow of methane and carbon dioxide mixtures at supersonic speeds in nozzles. In the simulations performed, the mixture reached conditions in which the carbon dioxide condensed while methane remained gaseous. With the simulation results, we analysed the impact of the nucleation phenomenon in the flow and could assess the sensitivity of the nucleation behaviour to variations of some flow parameters, such as total pressure, total temperature, and carbon dioxide concentration at the inlet. These results constitute a first analysis of the purification capacity of the supersonic gas separator by the condensation of carbon dioxide.*

Keywords: *Supersonic separator, Compressible flow, Nucleation, Multiphase flow, Numerical simulation*

1. INTRODUCTION

With the growth of the biogas production and pre-salt oil wells exploration, gas streams rich in methane but also with high concentration of impurities, as carbon dioxide, are available. To use those streams as energy source in applications such as vehicles or even for injection in the gas distribution network, the gas composition must meet the regulatory agency requirements (ANP requirements in the case of Brazil). Therefore, purification technologies need to be applied to remove the impurities of the fuel streams mentioned above.

When the impurities of these gas streams are analysed, it can be seen that the carbon dioxide is the most abundant, as it is usually the second species in terms of molar fraction of all gas components. Hence, methods of extracting the carbon dioxide from streams turn to be extremely relevant. Many developments happened in the last decades and nowadays the technologies that are more advanced are highlighted in Table 1.

Table 1. Purification methods comparison.

Purification method	Technology maturity	Purification level	Roubustness
Absorption	Very high	Very fine	Medium
Adsorption	Low	Fine	Low
Membranes	High	Fine	Low
Cryogenic	Medium	Coarse	High

In this paper we focus on the study of the principles of modelling one of the cryogenic separation methods, which is the supersonic separator. This device is composed of a nozzle, a swirl generator and a collector. A example of one of

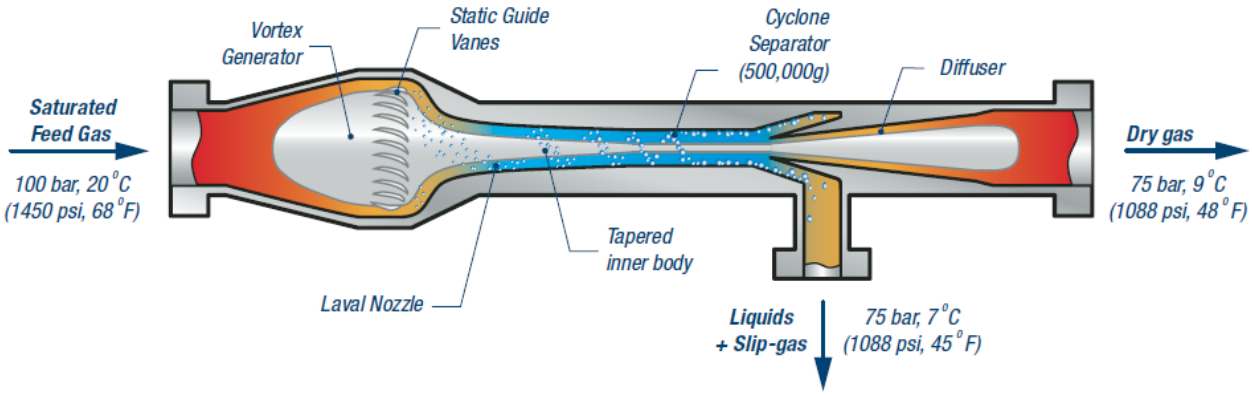

Figure 1. Schematic diagram of the Twister supersonic separator (Prast *et al.*, 2006)

these devices is the Twister supersonic separator, which is schematically represented in Figure 1. Here we investigate the nozzle of the device, and employ a numerical model to perform a first estimate of its capabilities of gas separation. This is possible because the nozzle is responsible for promoting the phase change of the carbon dioxide, and because only the condensed impurities can be separated. So we can determine the maximum raise of the fraction of the desired component, which is methane in this application.

To address the problem of modelling the supersonic separator some recent works (Bian *et al.*, 2018; Sun *et al.*, 2017) have used the two-dimensional analyses of the flow, but the thermodynamic models they employed presented a number of issues. In this paper, we propose a one-dimensional model to study the flow behaviour which accounts for the real gas behaviour of mixtures, and focus on delivering solid results with respect to the thermodynamic aspects.

2. METHODOLOGY

The model of the nozzle is based on the simplification of the Euler equations for compressible flow (Christodoulou and Miao, 2012) considering that the variations of the flow variables occur predominantly in the stream-wise direction. Therefore, we reduce the original set of equations from three-dimensional to one-dimensional and add some new terms to account for the variation of area of the nozzle. In the end, we obtain the following system of partial differential equations (PDEs) for a one dimensional compressible flow,

$$\frac{\partial}{\partial t}\begin{bmatrix}\rho\\ \rho u\\ \rho E\end{bmatrix}+\frac{\partial}{\partial x}\begin{bmatrix}\rho u\\ \rho u^2+p\\ \rho u H\end{bmatrix}=\frac{\partial}{\partial x}\ln A\begin{bmatrix}\rho u\\ \rho u^2\\ \rho u H\end{bmatrix}, \tag{1}$$

where ρ, u, p, E, H, A and x are, respectively, the density, velocity, static pressure, total internal energy, total enthalpy, area of the cross section and the axial position.

However, this system of equations is not sufficient to model all the phenomena found in the device that we want study, because it does not include phase change (condensation). So we performed a review of several liquid droplet nucleation models found in the literature, especially those applicable for compressible fluid flows in nozzles. The main models used in the literature are shown next.

2.1 Condensation modelling

In the literature, two additional quantities are calculated in order to have all the relevant variables of a compressible flow with condensation. The two variables are nucleation rate and the droplet radius growth rate. In this section we will first explore the nucleation models and next the radius growth models.

By using the classical nucleation theory (CNT) (Kalikmanov, 2013), we can see that the nucleation rate is given by

$$J=\sqrt{\frac{2\sigma_\infty}{\pi m_1}}\frac{\rho^V p^V}{\rho^l k_B T}\exp\left(-\frac{4}{27}\frac{\theta_\infty^3}{\ln S^2}\right), \tag{2}$$

where σ_∞ is the surface tension between vapour and liquid phase, m_l is the weight of one molecule of the liquid phase, ρ^V is the density of the vapour phase, p^V is static pressure of the vapour phase, ρ^l is the density of liquid phase, k_B is the Boltzmann constant, T is temperature, Θ_∞ is the non-dimensional surface tension and S is the saturation ratio.

Different from the other variables that are direct thermodynamic properties of the flow, the adimensional surface tension is defined as

$$\Theta_\infty=\frac{\sigma_\infty s_1}{k_B T}, \tag{3}$$

and the saturation ratio as

$$S = \exp\left[\frac{\mu^V(p^V, T) - \mu_{sat}(T)}{k_B T}\right], \tag{4}$$

where s_1 is

$$s_1 = (36\pi)^{1/3}(v^l)^{2/3}, \tag{5}$$

v^l is the theoretical volume of one molecule, μ^V the vapour chemical potential and μ_{sat} the vapour chemical potential at the saturated equilibrium state.

Some inconsistencies between the experimental results and the model showed the need of correcting the original model of the classical nucleation theory (Kalikmanov, 2013). Because of that, two additional nucleation rate models were are listed here so a analysis of the difference between all models results can be carried out to ensure that the most accurate nucleation model is applied. The first model is the internally consistent classical nucleation theory (ICCT), for which the nucleation rate that is calculated as

$$J_{ICCT} = \frac{1}{S}\sqrt{\frac{2\sigma_\infty}{\pi m_1}}\frac{\rho^V p^V}{\rho^l k_B T}\exp\left(\theta_\infty - \frac{4}{27}\frac{\theta_\infty^3}{\ln S^2}\right). \tag{6}$$

The second is the classical nucleation theory with the non isothermal correction applied (NISOCNT) (Kantrowitz, 1951), which is given by the equation

$$J_{NISOCNT} = \left(\frac{1}{1+\epsilon}\right) J_{CNT}, \tag{7}$$

where,

$$\epsilon = 2\frac{\gamma - 1}{\gamma + 1}\frac{h_{lv}}{RT_v}\left(\frac{h_{lv}}{RT_v} - 0.5\right), \tag{8}$$

γ is the ratio of specific heat, R the universal gas constant and h_{lv} the condensation enthalpy.

In the context of the droplet radius growth rate model, two models are commonly found in the literature. The first one is the Gyarmarthy model (Gyarmathy, 1962),

$$\frac{\partial r}{\partial t} = \frac{\lambda_v\left(1 - \frac{r^*}{r}\right)(T_s - T)}{\rho_l h_{lv} r\left(1 + 3.18\frac{Kn}{Pr}\right)}. \tag{9}$$

The other model is that presented by Young (Young, 1980), and expresses the radius growth rate as

$$\frac{\partial r}{\partial t} = \frac{\lambda_v\left(1 - \frac{r^*}{r}\right)(T_s - T)}{\rho_l h_{lv} r\left[\frac{1}{1+2\beta Kn} + (1-\nu)3.78\frac{Kn}{Pr}\right]}. \tag{10}$$

In the equations above, r is the droplet radius, t is time, λ_v is the vapour thermal conduction coefficient, r^* is the critical droplet radius, T_s is the saturation temperature, Pr is the Prandtl number, Kn is the Knudsen number and β and ν are and model calibration coefficients.

2.2 System of PDEs for modelling a supersonic separator

To complete the system of equations (1) so it can handle two-phase flow, it is necessary to add additional terms in order to account for the condensate in the flow. For that, the method of momenta was applied as presented by Put (2003). Consequently, the number of equations goes from 3 to 7 and the final system becomes

$$\frac{\partial}{\partial t}\begin{bmatrix}\rho\\ \rho u\\ \rho E\\ \rho Y\\ \rho Q_2\\ \rho Q_1\\ \rho Q_0\end{bmatrix} + \frac{\partial}{\partial x}\begin{bmatrix}\rho u\\ \rho u^2 + P\\ \rho u H\\ \rho u Y\\ \rho u Q_2\\ \rho u Q_1\\ \rho u Q_0\end{bmatrix} - \frac{\partial}{\partial x}\ln A\begin{bmatrix}\rho u\\ \rho u^2\\ \rho u H\\ \rho u Y\\ \rho u Q_2\\ \rho u Q_1\\ \rho u Q_0\end{bmatrix} = \begin{bmatrix}0\\ 0\\ 0\\ \frac{4}{3}\pi\rho_l\left(Jr^{*3} + 3\rho Q_2\frac{d\bar{r}}{dt}\right)\\ Jr^{*2} + 2\rho Q_1\frac{d\bar{r}}{dt}\\ Jr^* + \rho Q_0\frac{d\bar{r}}{dt}\\ J_c\end{bmatrix}. \tag{11}$$

In this model we have momenta of different order, Q_i, which are scalars used to represent the droplet radius distribution effect without the need of calculating the radius of each group of droplets that are formed in the domain. Therefore, Q_0, Q_1, Q_2 and Y, which is a substitute for Q_3 in equation 11, are scalars that can be read as the number of droplets, the radius of the droplets, the surface area of all droplets and the volume of all the droplets, respectively. This became more evident as the source terms in the right hand-side of equation 11 are analysed. In this approach, as if a root mean square of the droplet radius were taken as the mean droplet radius, we have the mean radius, by definition, as,

$$r = \sqrt{\frac{Q_2}{Q_0}}. \tag{12}$$

2.3 Equation of state and thermophysical properties

To ensure closure to the problem a equation of state must be defined. In this work we selected the Peng-Robinson equation of state which is defined as

$$p = \frac{RT}{v-b} + \frac{a}{(v+\Delta_1 b)(v+\Delta_2 b)}. \tag{13}$$

This equation is already implemented in the CoolProp thermophysical library (Bell and Jager, 2016), used in this work.

Another important variable to the nucleation problem is the surface tension. We used one expression for water surface tension,

$$\sigma = 235.8\left(1-\frac{T}{T_c}\right)^{1.256}\left[1-0.625\left(1-\frac{T}{T_c}\right)\right], \tag{14}$$

And a second expression for other species,

$$\sigma = kT_c\left(\frac{N_a}{V_c}\right)^{2/3}(4.35+4.14\omega)\left(1-\frac{T}{T_c}\right)^{1.26}\left[1+0.19\left(1-\frac{T}{T_c}\right)^{0.5}-0.487\left(1-\frac{T}{T_c}\right)\right]. \tag{15}$$

where T_c and ω are the critical temperature and the acentric factor.

Finally, the thermal conductivity must be determined and for that we use,

$$\lambda_m = \frac{\lambda_1 x_1}{x_1 + A_{12}x_2} + \frac{\lambda_2 x_2}{x_2 + A_{21}x_1}, \tag{16}$$

Where,

$$A_{ij} = \frac{1.065}{\sqrt{2^3}}\frac{\left[1+\sqrt{\frac{\lambda_i^0}{\lambda_j^0}}\sqrt[4]{\frac{M_i}{M_j}}\right]^2}{\left(1+\frac{M_i}{M_j}\right)^{1/2}}. \tag{17}$$

and M is the molar mass of the specie.

We also employed the Stiel-Thodos (Stiel and Thodos, 1964) correction expression, which allow us to correct the thermal conductivity as a function of the pressure, that is,

$$(\lambda_m - \lambda_m^0)\zeta_m z_{cm}^5 = 14.0\times10^{-8}\left(e^{0.535\rho_{rm}}-1\right), \text{ if } \rho_{rm} < 0.5, \tag{18}$$

where,

$$\rho_{rm} = \frac{\rho_m}{\rho_{cm}}, \tag{19}$$

$$\zeta_m = \frac{T_{cm}^{1/6} M_m^{1/2}}{P_{cm}^{2/3}}, \tag{20}$$

and,

$$z_{cm} = 0.291 - 0.08\omega_m = 0.291 - 0.08\sum x_i\omega_i. \tag{21}$$

2.4 Numerical Scheme

In order to solve the system of PDEs, equation (11), the AUSMDV split flux method was implemented according to Wada and Liou (1994). The interface flux between two elements is defined in the AUSM scheme by

$$F_{1/2} = \frac{1}{2}\left[(\rho u)_{1/2}(\Psi_L + \Psi_R) - |(\rho u)_{1/2}|(\Psi_R - \Psi_L)\right] + p_{1/2}, \tag{22}$$

where

$$\Psi = \begin{bmatrix} 1 & u & H & Y & Q_2 & Q_1 & Q_0 \end{bmatrix}^t, \tag{23}$$

and

$$P_{1/2} = \begin{bmatrix} 0 & p_{1/2} & 0 & 0 & 0 & 0 & 0 \end{bmatrix}^t. \tag{24}$$

In addition, the momentum in the interface, $(\rho u)_{1/2}$, is

$$(\rho u)_{1/2} = \frac{1}{2}(1+s)(\rho u^2)_{AUSMV} + \frac{1}{2}(1-s)(\rho u^2)_{AUSMD}, \tag{25}$$

where

$$s = \frac{1}{2}\min\left(K\frac{|p_R - p_L|}{\min(p_L, p_R)}\right), \tag{26}$$

$$(\rho u^2)_{AUSMV} = u_L^+(\rho u)_L + u_R^-(\rho u)_R, \tag{27}$$

and

$$(\rho u^2)_{AUSMD} = \frac{1}{2}[(\rho u)_{1/2}(u_L + u_R) - |(\rho u)_{1/2}|(u_R - u_L)]. \tag{28}$$

In these expressions, u_L^+ e u_R^- are

$$u_L^+ = \begin{cases} \alpha_L \frac{(u_L + c_m)^2}{4c_m} + (1-\alpha_L)\frac{u_L + |u_L|}{2} & \text{if } |u_L| \le c_m, \\ \frac{u_L + |u_L|}{2} & \text{other cases,} \end{cases} \tag{29}$$

$$u_R^- = \begin{cases} \alpha_R - \frac{(u_R - c_m)^2}{4c_m} + (1-\alpha_R)\frac{u_R - |u_R|}{2} & \text{if } |u_R| \le c_m, \\ \frac{u_R - |u_R|}{2} & \text{other cases.} \end{cases} \tag{30}$$

In equations (29) and (30) the α_L, α_R and c_m factors are defined as

$$\alpha_L = \frac{2(p/\rho)_L}{(p/\rho)_L + (p/\rho)_R} \quad , \quad \alpha_R = \frac{2(p/\rho)_R}{(p/\rho)_L + (p/\rho)_R} \quad , \quad c_m = \max(c_L, c_R). \tag{31}$$

In equation (22), $p_{1/2}$ is calculated by

$$p_{1/2} = p_L^+ + p_R^-, \tag{32}$$

where

$$p_L^+ = \begin{cases} p_L \frac{(u_L + c_m)^2}{4c_m^2}\left(2 - \frac{u_L}{c_m}\right) & \text{if } |u_L| \le c_m, \\ p_L \frac{u_L + |u_L|}{2u_L} & \text{other cases,} \end{cases} \tag{33}$$

$$p_R^- = \begin{cases} p_R \frac{(u_R - c_m)^2}{4c_m^2}\left(2 + \frac{u_R}{c_m}\right) & \text{if } |u_R| \le c_m, \\ p_R \frac{u_R - |u_R|}{2u_R} & \text{other cases.} \end{cases}. \tag{34}$$

In this scheme, we still have to apply a specific correction in the element at which the subsonic-supersonic transition occurs. For that we define two cases,

$$\begin{cases} \text{Case A: } u_L - c_L < 0 \text{ and } u_R - c_R > 0, \\ \text{Case B: } u_L - c_L > 0 \text{ and } u_R - c_R < 0. \end{cases}. \tag{35}$$

With the cases defined, we apply the correction as follows:

$$\begin{cases} \text{If only case A: } F_{1/2,E-Fix} = F_{1/2} - C\Delta(u-c)\Delta(\rho\Psi), \\ \text{If only case B: } F_{1/2,E-Fix} = F_{1/2} - C\Delta(u+c)\Delta(\rho\Psi). \end{cases} \tag{36}$$

In equation (36), $\Delta() \equiv ()_R - ()_L$ and $C = 0.125$. We employed a first-order Euler temporal scheme with a CFL of 0.5 and the spatial discretization of 1000 uniform cells along the nozzle axis. All those calculations were carried out by a Python script made by the first author.

3. Results

The objective of the model is to predict the behaviour of multi-phase, multi-component flows through nozzles. However, first a validation step must be carried out.

3.1 Model Validation

In the validation of the model we used experimental results from experiments by Moses and Stein (1978). The nozzle geometry used in the experiments is presented in Figure 2. Two cases of experiments were chosen to validate the model. The boundary conditions of those two experiments are shown in Table 2.

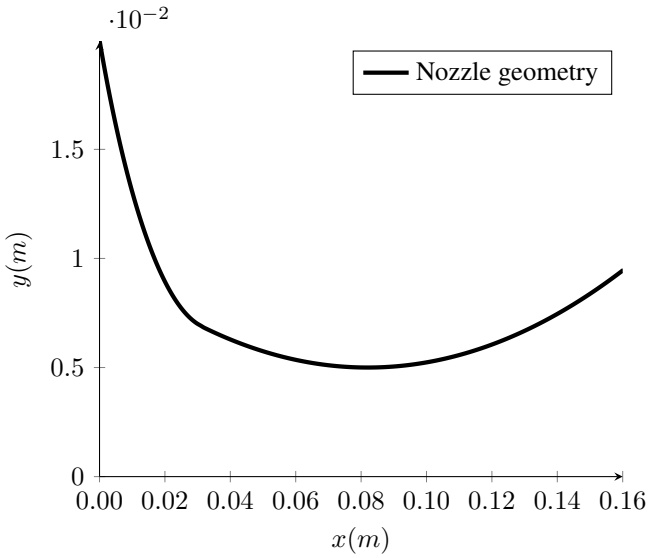

Figure 2. Nozzle geometry used for validation (Moses and Stein, 1978).

Table 2. Table of boundary conditions of the simulation carried out to reproduce the experiments of Moses and Stein (Moses and Stein, 1978).

Case	P_0[Pa]	T_0[K]
424	41903	376
193	43032	366

Figure 3 shows the results we obtained for case 193. With those results we concluded that the NISOCNT model was the most suitable for the case. A comparison between the two models of droplet radius growth rate and the experimental results is also shown in the same figure.

We also have analysed the results of case 424 but only for the NISOCNT nucleation model. The pressure field and relative error are shown in Figure 4. From the error graphs of Figures 3 and 4 it is possible to conclude that the two droplet radius growth rate models predict well the phenomenon when the NISOCNT nucleation model is applied. However, as the Gyamarty model has simplifications that makes it specific for water, we use the Young model to make the next analyses.

3.2 Monocomponent simulation

To analyse the monocomponent nucleation behaviour, we use a geometry proposed by Sun *et al.* (2017) shown in figure 5. As an exploratory analysis, we predict the flow behaviour for different conditions in order to see mainly the effect of changes in boundary conditions over the condensation phenomenon. We used the boundary conditions listed in Table 3 so we can verify the changes that the total pressure in the inlet of the nozzle has on the nucleation process.

As we intend to verify the maximum capacity of condensation of the device, we plot in Figure 6 the condensate mass fraction as a function of the position. We can see that, as the pressure is increased, the condensation wave takes place earlier and the mass fraction of condensate at the nozzle exit is higher.

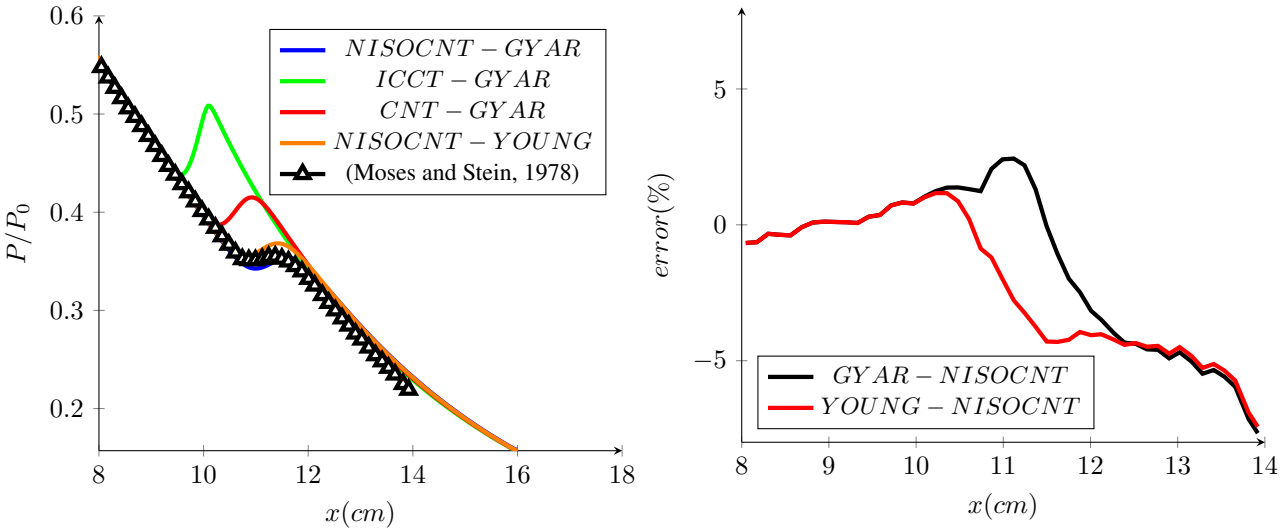

Figure 3. Comparison of pressure field between experimental data and results of different nucleation models for wet steam and relative error of NISOCNT model with the Gyarmarthy (GYAR) and Young (YOUNG) radius growth models - Moses and Stein, case 193.

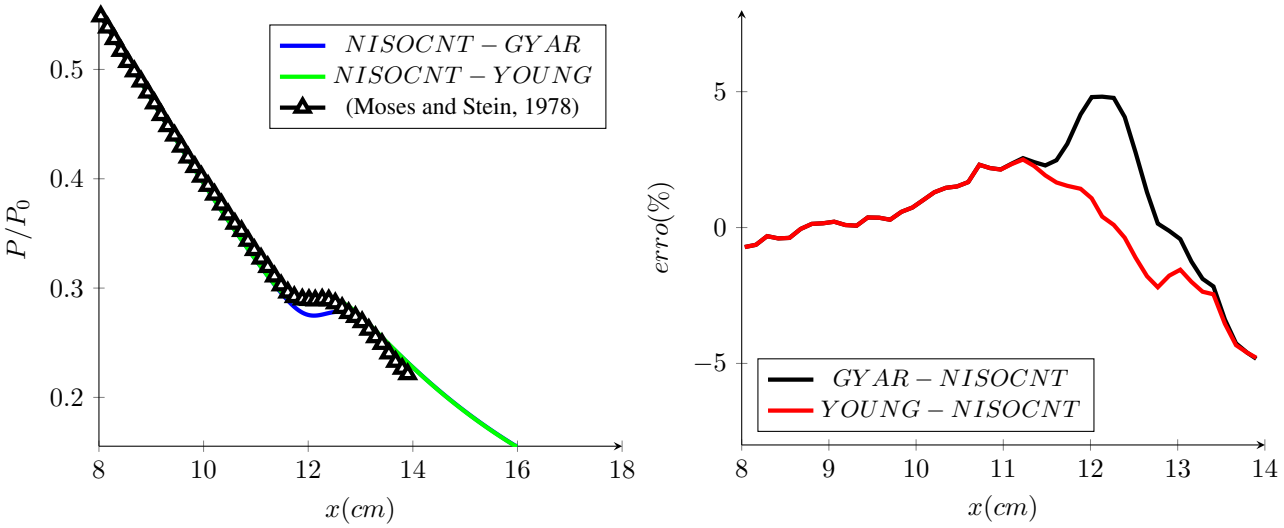

Figure 4. Comparison of pressure field between experimental data and results of NISOCNT nucleation model for wet steam and relative error of NISOCNT model with the Gyarmarthy (GYAR) and Young (YOUNG) radius growth models - Moses and Stein, case 424.

Table 3. Boundary conditions for monocomponent (CO_2) flow simulations.

P_0[MPa]	T_0[K]
2.25	293.15
2.00	293.15
1.75	293.15

3.3 Two-component simulation

To be closer to the fluid of the final application, we carried out results of the flow of a mixture of CH_4 and CO_2 through the same nozzle (see Figure 5). The boundary conditions employed in the simulations were those in Table 4. The results of methane molar fraction in the simulation of two-component are shown in Figure 7. As the methane molar fraction curve presents an asymptotic behaviour in each case, we conclude that more than one step is necessary in order achieve higher molar fractions of CH_4 if a low initial CH_4 molar fraction is imposed. In the results of Figure 7 it is possible to see that if we desire to upgrade a stream that initially was with 70% of CH_4 molar fraction to 90% of CH_4, we would need, at least, 3 expansion processes if we consider that all condensate is extracted from the main stream.

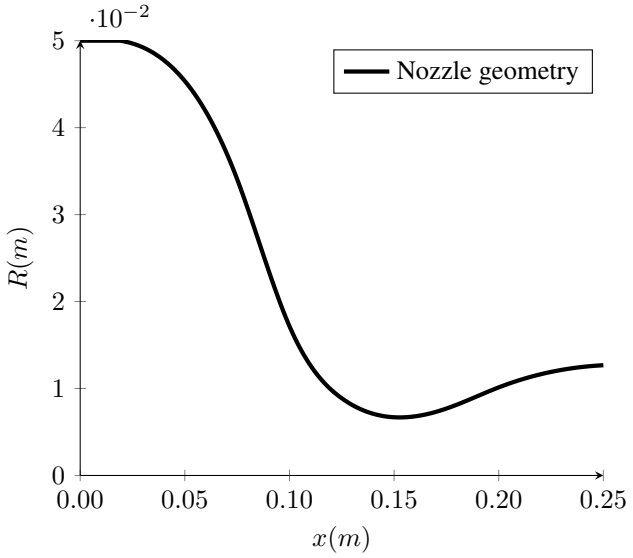

Figure 5. Nozzle geometry for flow analyze (Sun *et al.*, 2017).

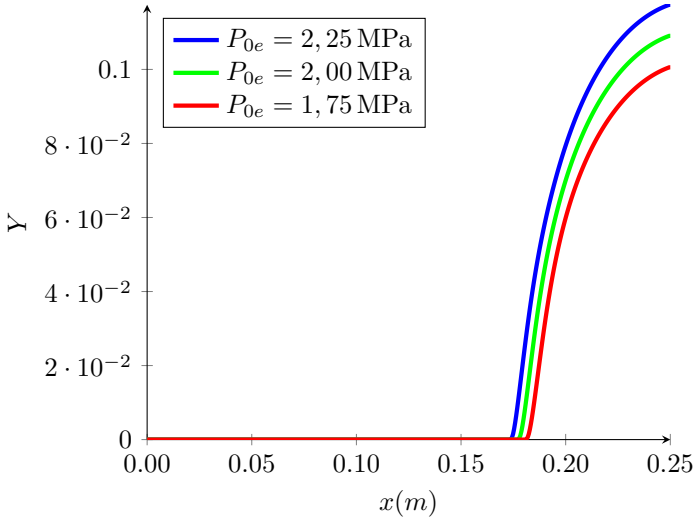

Figure 6. Condensate mass fraction in CO_2 flow with condensation varying total pressure in nozzle inlet.

Table 4. Boundary conditions for the two-component flows.

Varying y_{CH_4}			Varying P_0		
$P_0[MPa]$	$T_0[K]$	y_{CH_40}	$P_0[MPa]$	$T_0[K]$	y_{CH_40}
6	293	0,9	6	293	0,7
6	293	0,8	5	293	0,7
6	293	0,7	4	293	0,7

4. CONCLUSIONS

The proposed model could reproduce the pressure field of the experimental data available in the literature for the water expansion in a convergent-divergent nozzle. The model was conceived so it can handle multicomponent flow, as long as just one specie can condensate.

In the expansion of carbon dioxide it was possible to see that the boundary conditions have major impact in the capacity of the device to condensate the fluid. In the tested case, the increase in pressure resulted in the raise of the fraction of condensate in the outlet of the nozzle.

In the expansion of mixtures of CH_4 and CO_2 the boundary conditions also play major role in the condensation capacity of the device. In the carried out analyses the change of CH_4 mole fraction and the pressure in the nozzle inlet had direct impact in the variation of mole fraction. The lower the CH_4 mole fraction the higher the mole fraction variation and the higher the pressure the higher the mole fraction variation. Another important information retrieved from the results is

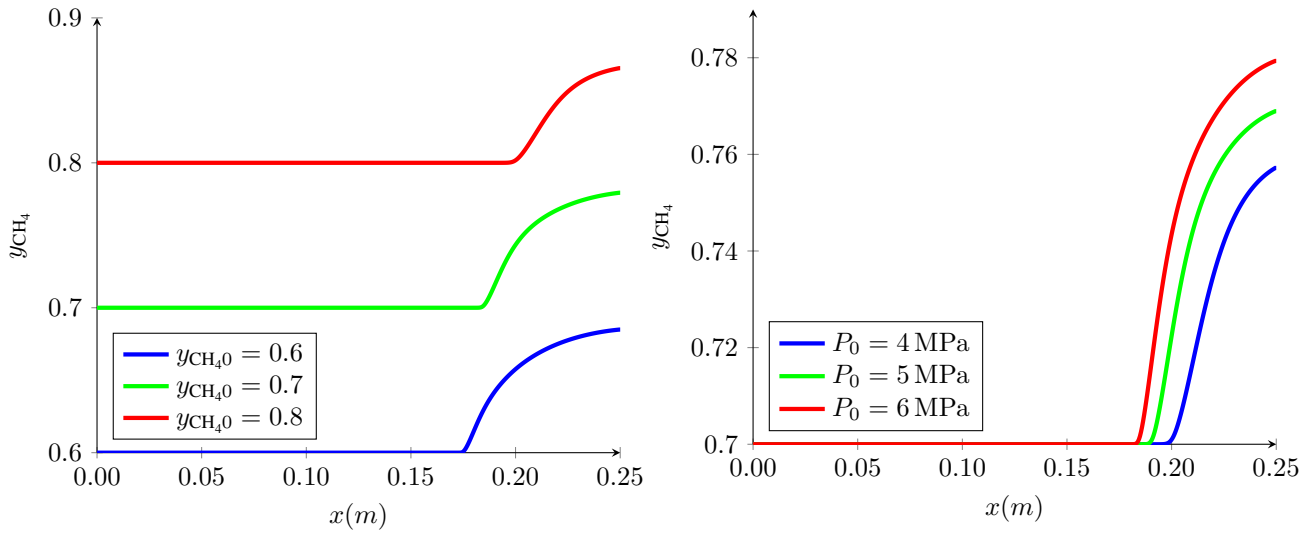

Figure 7. CH_4 molar fraction in the gas phase field in a CH_4-CO_2 flow varying the gas composition in the nozzle inlet.

that the CH_4 mole fraction exhibits an asymptotic behaviour. Therefore it is not possible to greatly reduce the CO_2 mole fraction of the mixture in a single expansion. In the simulations carried out, the variation of CO_2 mole fraction ranged from 5% to 10%.

Finally, the quasi-one-dimensional model presented itself as a valuable tool to model the flow with homogeneous condensation. Therefore, an initial optimisation of the nozzle profile using the described model is possible to enhance the capacity of the nozzle to generate condensate, as well as an exploration of the optimum boundary conditions for the nozzle.

5. ACKNOWLEDGEMENTS

We acknowledge Clark Solutions, Shell, FAPESP, and USP for all support that made this research possible. We gratefully acknowledge support of the RCGI – Research Centre for Gas Innovation, hosted by the University of São Paulo (USP) and sponsored by FAPESP – São Paulo Research Foundation (2014/50279-4) and Shell Brasil, and the strategic importance of the support given by ANP (Brazil's National Oil, Natural Gas and Biofuels Agency) through the R&D levy regulation. B. A. Avancini thanks Clark Solutions for financial support to the research. B. S. Carmo thanks the Brazilian National Council for Scientific and Technological Development (CNPq) for financial support from in the form of a productivity grant, number 312951/2018-3.

6. REFERENCES

Bell, I.H. and Jager, A., 2016. "Helmholtz energy transformations of common cubic equations of state for use with pure fluids and mixtures". *Journal of Research of the National Institute of Standards and Technology*, Vol. 121, p. 238. doi:10.6028/jres.121.011. URL `https://doi.org/10.6028/jres.121.011`.

Bian, J., Jiang, W., Hou, D., Liu, Y. and Yang, J., 2018. "Condensation characteristics of ch 4 -co 2 mixture gas in a supersonic nozzle". *Powder Technology*, Vol. 329, pp. 1–11. doi:10.1016/j.powtec.2018.01.042. URL `https://doi.org/10.1016/j.powtec.2018.01.042`.

Christodoulou, D. and Miao, S.X., 2012. "Compressible flow and euler's equations". *arXiv: Analysis of PDEs*.

Gyarmathy, G., 1962. *Grundlagen einer Theorie der Nassdampfturbine*. Ph.D. thesis, ETH Zurich, Zurich. doi: 10.3929/ethz-a-000087803. Mitteilungen aus dem Institut fÃ¼r thermische Turbomaschinen an der ETH, Nr.6. Diss. Techn.Wiss. ETH Zurich, Nr. 3221, 0000. Ref.: Traupel, W. ; Korref.: Ackeret, J..

Kalikmanov, V., 2013. *Nucleation Theory*. Springer Netherlands. doi:10.1007/978-90-481-3643-8. URL `https://doi.org/10.1007/978-90-481-3643-8`.

Kantrowitz, A., 1951. "Nucleation in very rapid vapor expansions". *The Journal of Chemical Physics*, Vol. 19, No. 9, pp. 1097–1100. doi:10.1063/1.1748482. URL `https://doi.org/10.1063/1.1748482`.

Moses, C.A. and Stein, G.D., 1978. "On the growth of steam droplets formed in a laval nozzle using both static pressure and light scattering measurements". *Journal of Fluids Engineering*, Vol. 100, No. 3, pp. 311–322. doi: 10.1115/1.3448672. URL `https://doi.org/10.1115/1.3448672`.

Prast, B., Lammers, B. and Betting, M., 2006. "CFD for supersonic gas processing". In *Fifth International Conference on CFD in the Process Industries*. CSIRO, Melbourne, Australia. URL

http://www.cfd.com.au/cfd_conf06/PDFs/027Pra.pdf.

Put, F., 2003. *Numerical Simulation of Condensation in Transonic Flows*. Ph.D. thesis, Universiteit Twente.

Stiel, L.I. and Thodos, G., 1964. "The thermal conductivity of nonpolar substances in the dense gaseous and liquid regions". *AIChE Journal*, Vol. 10, No. 1, pp. 26–30. doi:10.1002/aic.690100114. URL https://doi.org/10.1002/aic.690100114.

Sun, W., Cao, X., Yang, W. and Jin, X., 2017. "Numerical simulation of co_2 condensation process from $ch_4 - co_2$ binary gas mixture in supersonic nozzles". *Separation and Purification Technology*, Vol. 188, pp. 238 – 249. ISSN 1383-5866. doi:https://doi.org/10.1016/j.seppur.2017.07.023. URL http://www.sciencedirect.com/science/article/pii/S138358661730196X.

Wada, Y. and Liou, M., 1994. "A flux splitting scheme with high-resolution and robustness for discontinuities". *32nd Aerospace Sciences Meeting and Exhibit*. doi:10.2514/6.1994-83.

Young, J.B., 1980. "Spontaneous condensation of steam in supersonic nozzles. Part 1: Nucleation and droplet growth theory. Part 2: Numerical methods and comparison with experimental results". NASA STI/Recon Technical Report N.

7. RESPONSIBILITY NOTICE

The authors are solely responsible for the printed material included in this paper.